DOI: 10.37190/abb/207864

Structural and biomechanical analysis of femurs from mice treated with diclofenac, miR-15b and miR-365

Tomasz P. Lehmann[1*], Aleksandra Trzaskowska[2], Ewa Pruszyńska-Oszmałek[3], Paweł Kołodziejski[3], Magdalena Wojtków[4], Celina Pezowicz[4], Sławomir Mielcarek[2], Agnieszka Hertel[1], Paweł P. Jagodzinski[1], Maciej Głowacki[5]

[1]Department of Biochemistry and Molecular Biology, Poznan University of Medical Sciences, Poznan, Poland

[2]Department of Physics of Nanostructures, ISIQ, Faculty of Physics, Adam Mickiewicz University, Poznan, Poland

[3]Department of Animal Physiology, Biochemistry and Biostructure, Poznan University of Life Sciences, Poznan, Poland

[4]Department of Mechanics, Materials and Biomedical Engineering, Faculty of Mechanical Engineering, Wroclaw University of Science and Technology, Wrocław, Poland

[5]Department of Paediatric Orthopaedics and Traumatology, Poznan University of Medical Sciences, Poznan, Poland

[*]Corresponding author: Tomasz P. Lehmann, Department of Biochemistry and Molecular Biology, Poznan University of Medical Sciences, Poznan, Poland, e-mail address:: tlehmann@ump.edu.pl

Submitted: 22nd March 2025

Accepted: 3rd July 2025

Authors' contributions

T.P.L. Preparation of the research program, statistical analysis, interpretation of data, preparation of the manuscript; A.T. Execution of the research, statistical analysis, interpretation of data; E.P. Execution of the research; P.K. Execution of the research; M.W. Execution of the research, statistical analysis, interpretation of data;C.P. Execution of the research, interpretation of data; S.M. Execution of the research, interpretation of data; A.H. Execution of the research, interpretation of data; P.P.J. Interpretation of data; M.G. Preparation of the research program, interpretation of data, obtaining funding.

Abstract

Purpose: Nonsteroidal anti-inflammatory drugs (NSAIDs) are used to treat pain, but they have side effects, including the inhibition of bone healing. Diclofenac (DF), a member of the NSAID group, affects bone health adversely. One potential approach to protect bones from the effects of NSAIDs involves the administration of short nucleic acids, such as microRNAs (miRNAs). This study aimed to determine whether two specific miRNAs, miR-15b and miR-365, could mitigate the effects of DF on bone.

Methods: We used the C57BL/6J mouse strain and the MC3T3-E1 preosteoblast cell line derived from this mouse strain. Female C57BL/6J mice were treated with DF and miR-15b or miR-365 mimics. After euthanising the mice, we analysed their femurs using micro-computed tomography (μCT) and dynamic mechanical analysis (DMA). In addition, we performed experiments in cultured MC3T3-E1 cells, which were transfected with either miR-15b or miR-365. We assessed the relative mRNA levels of osteoblast differentiation markers using real-time PCR.

Results: Our findings indicated that miR-15b and miR-365 were effective in reversing the detrimental effects of DF on bone mineral density. DF decreased the bone's storage modulus (E'), while miR-15b and miR-365 ameliorated this effect. In the preosteoblast MC3T3-E1 cells, DF did not significantly regulate marker genes; however, the administration of miR-15b and miR-365 reduced the gene expression of *Runx2*, *Alp*, and *Satb2*.

Conclusions: In summary, the impact of DF on the structural and mechanical properties of bone was not mediated by gene regulation in osteoblasts. However, osteoblasts were responsive to the administration of miR-15b and miR-365.

Keywords: miRNA, femur, bone microstructure, preosteoblast, dynamic mechanical analysis.

Introduction

Nonsteroidal anti-inflammatory drugs (NSAIDs) are widely utilised to alleviate pain originating from the musculoskeletal system, including pain caused by fractures or tumours. These agents are prescribed for both acute and chronic pain management, often following orthopaedic injuries or cancer-related interventions, providing substantial relief to patients [1]. Despite their therapeutic utility, NSAIDs are associated with adverse effects that extend beyond the musculoskeletal tissues. Among them, diclofenac (DF), a commonly used NSAID, is particularly noted for its effectiveness in treating chronic skeletal pain. DF (sodium 2-(2,6-dichloroanilino)-phenylacetate), a derivative from the aryl acetic acid group, is a non-selective inhibitor of cyclooxygenase enzyme. By targeting both COX-1 and COX-2 isoforms, DF interferes with the function of osteoblasts, osteoclasts, and macrophages, thereby impairing the early phases of bone regeneration [2]. While the inhibition of COX-1 disrupts the synthesis of homeostatic prostaglandins, COX-2 suppression interferes with prostaglandin production at inflammatory sites. Long-term administration of NSAIDs has been implicated in delayed bone repair and weakening of the skeleton [3]. Recent studies have also explored the potential of miRNAs to counteract such detrimental effects [4].

MicroRNAs (miRNAs) are short RNA sequences, typically 20 nucleotides long, which exert regulatory control over gene expression at the post-transcriptional level by binding to complementary seed sequences in the 3'-untranslated regions (3'-UTRs) of target mRNAs. In biomedical research, miRNAs are increasingly employed as modulators of gene function and potential therapeutic agents [5]. Numerous investigations have identified miRNAs as critical regulators of bone metabolism, prompting our focus on two underexplored molecules—miR-15b and miR-365—both influencing bone-related processes.

miR-15b-5p has been shown to target vascular endothelial growth factor α (*Vegfa*) in hypertrophic chondrocytes derived from Balb/c mice [6]. VEGF secreted by these cells plays an integral role in vascularisation, ossification, and cartilage remodelling [6]. In addition, miR-15b modulates the transforming growth factor β (TGF-β) signalling pathway, which regulates the osteogenic differentiation of bone marrow stromal cells (BMSCs). miR-15b promotes an increase in Smad2/3 activity by downregulating their inhibitory Smad7, which in turn upregulates Runx2 gene expression [7]. Furthermore, miR-15b inhibits Smurf1, a SMAD-specific E3 ubiquitin ligase safeguarding osteogenic differentiation pathways [8].

miR-365 is implicated in regulating osteoclast formation, modulating these cells' size and number. During osteoclastogenesis, miR-365 levels rise, slowing proliferation while supporting cell survival [9]. Similar increases in miR-365 have been recorded during

osteoblast differentiation in B6 and C3H mouse strains [10]. This miRNA also mitigates the suppressive impact of dexamethasone (DEX) on osteoblast viability and function through the regulation of histone deacetylase 4 (HDAC4) expression [11]. miR-365, recognised as mechanoresponsive, also contributes to chondrocyte differentiation and hypertrophy [12].

Recent findings highlight that miR-365-2-5p, delivered via exosomes from M2 macrophages, targets olfactomedin-like 1 (OLFML1), a gene whose downregulation facilitates osteoblast mineralisation [13]. M2 macrophages possess a reparative phenotype that is crucial for skeletal regeneration [13]. OLFML1, highly expressed in osteoblast-rich tissues during development, is essential for proper mineralisation [14]. Moreover, in cartilage-derived stem cells from osteoarthritis (OA) patients, miR-365 has been implicated in regulating differentiation pathways associated with OA pathology [15].

Despite the growing literature on the independent roles of NSAIDs and miRNAs in bone biology, their combined influence on bone structure and function remains largely underexplored. Previously, we reported that DF caused a reduction in bone mineral density (BMD) in mouse femurs [16]. As NSAIDs continue to be linked to skeletal degradation, identifying a molecular strategy to mitigate these effects remains a priority. Thus, we aimed to assess whether miR-15b and miR-365 could offer protection against DF-induced skeletal damage.

This study investigates the potential of miR-15b and miR-365 to offset some of the adverse skeletal effects associated with DF treatment. To this end, we employed a dual-model approach utilising both in vivo (C57BL/6J mice) and in vitro (MC3T3-E1 cells) derived from the same strain. In the animal model, mice received daily DF injections alongside weekly administration of miR-15b or miR-365 for four weeks. Post-treatment, femoral bones were examined via microcomputed tomography (μCT) and dynamic mechanical analysis (DMA). Parallel in vitro experiments involved transfecting MC3T3-E1 cells with either miRNA and exposing them to DF, followed by RT-qPCR analysis of osteogenic marker genes. Although DF alone had no substantial effect on gene expression, co-treatment with miR-15b or miR-365 led to a significant downregulation of key osteogenic genes.

Materials and methods

Animals

The experimental procedures involving animals were approved by the Local Ethical Commission for Animal Research at the Poznań University of Life Sciences (Permission No. 39/2017). All protocols complied with the ARRIVE guidelines and were carried out in the

Department of Animal Physiology, Biochemistry and Biostructure, Poznań University of Life Sciences [17]. A total of 96 female C57BL/6J mice, aged 12 weeks, were used in this study. The animals, obtained from the Mossakowski Medical Research Centre of the Polish Academy of Sciences in Warsaw, were housed in standard polycarbonate cages under stable environmental conditions (21 ± 1 °C; 12-hour light/dark cycle), with unlimited access to water and Labofeed B chow (Kcynia, Poland). Before starting the experiment, mice underwent a two-week acclimatisation period to adjust to the laboratory environment. Using female animals was intentional, based on existing data indicating a higher prevalence of osteoporosis in females.

The animals were randomly assigned into eight experimental groups (n = 12 per group): Control, DF, NEG (negative control miRNA), NEG + DF, miR-15b, miR-15b + DF, miR-365, and miR-365 + DF. Mice in the DF-treated groups received daily intraperitoneal injections of diclofenac sodium (5 mg/kg/day; Alfa Aesar, cat. no. J62609, Haverhill, MA, USA) for 30 consecutive days. Control animals were administered an equivalent volume of physiological saline (0.9% NaCl).

Mice assigned to the NEG, NEG + DF, miR-15b, miR-15b + DF, miR-365, and miR-365 + DF groups were treated with miRNA mimics, administered once per week via *in vivo* transfection using JetPEI reagent (Polyplus, Illkirch, France), following the manufacturer's protocol. The injected oligonucleotides included: mmu-miR-15b-5p (Thermo Fisher Scientific, Catalog no: 4464070, Assay ID: MC10904), mmu-miR-365-3p (Catalog no: 4464070, Assay ID: MC11133), negative control (mirVana™ miRNA Mimic Negative Control #1, 4464061). Each mouse received 5 µg of miRNA, dissolved in 25 µl of 10% glucose and diluted with sterile water to a total volume of 50 µl. In parallel, 0.6 µl of JetPEI reagent was also prepared in 25 µl of 10% glucose and diluted to 50 µl. These solutions were combined, mixed gently, and incubated for 15 minutes at room temperature. The final 100 µl complex was administered via subcutaneous injection.

After 30 days, the experiment was concluded. Animals were sacrificed by decapitation, and both femurs were carefully excised. Any remaining soft tissues were meticulously removed using sterile scalpels. Bones were rinsed in PBS, gently dried with filter paper, wrapped in aluminium foil, and stored in sealed tubes at –20°C until further analysis.

Microtomography examination

The evaluation of microarchitecture in both cortical and trabecular regions of the distal right femur in mice was carried out using the SkyScan 1172 high-resolution micro-CT scanner

(Bruker, Belgium). A total of 96 femoral samples (12 per experimental group) were scanned at 6 µm resolution, using standardised settings: 181 µA tube current, 55 kV voltage, 0.5 mm aluminium filter, and an 800 ms exposure time. During the scanning process, samples were carefully wrapped in moist paper tissue, inserted into polypropylene tubes, and stabilised using foam supports to minimise movement and desiccation. To quantify bone mineral density (BMD), calibration phantoms provided by Bruker containing calcium hydroxyapatite (CaHA) at concentrations of 0.25 and 0.75 g/cm³ were employed. Image reconstruction was performed using NRecon software (Bruker), and morphometric analysis was conducted in defined volumes of interest (VOIs) using CtAn software (Bruker). VOIs were precisely located relative to the growth plate, which was visually identified in each sample using cross-sectional image data (Figure 1).

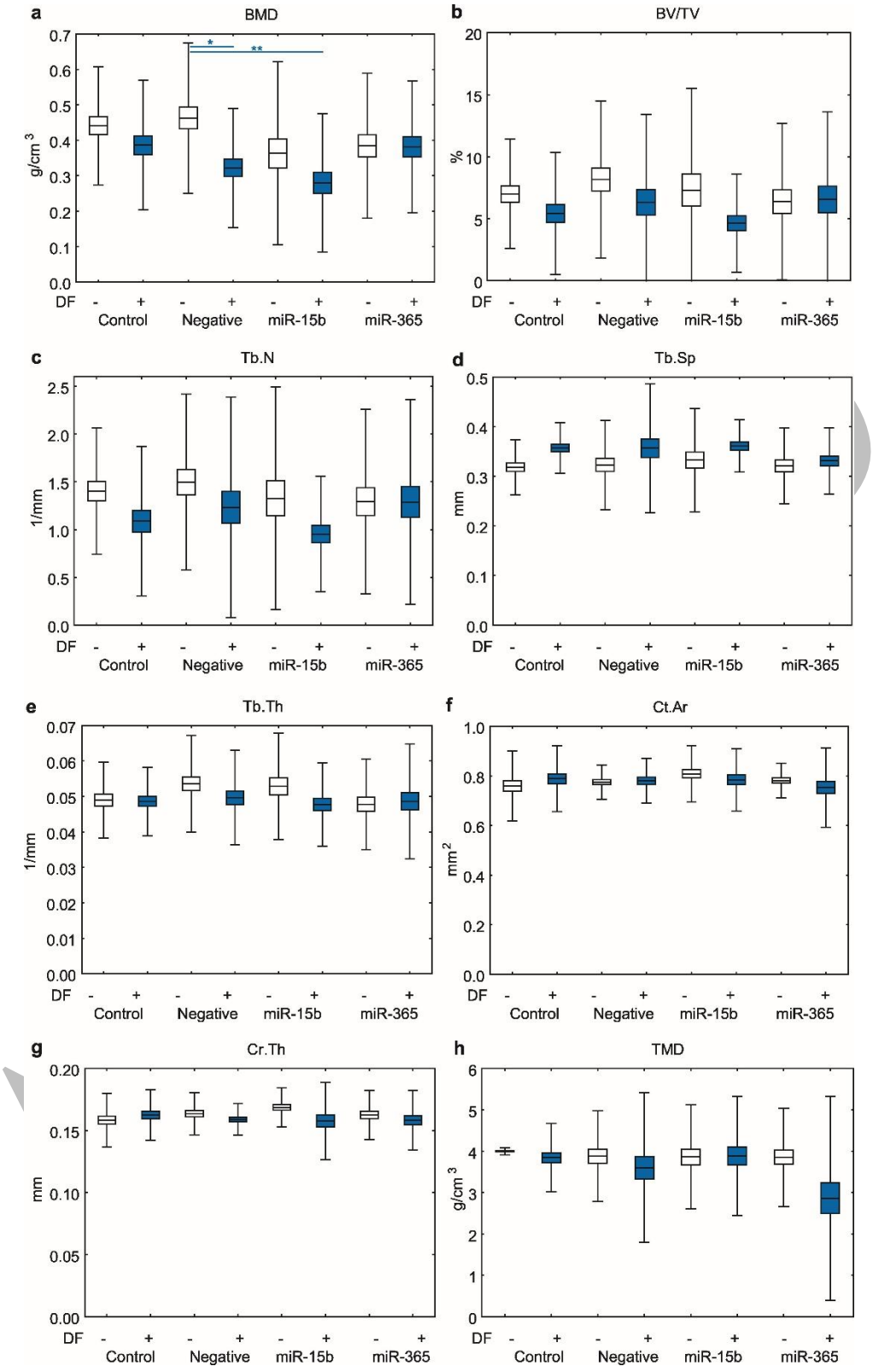

Fig.1 Mouse femur analysis by microcomputer tomography; Structural parameters BMD (a), BV/TV (b), TbN (c), TbSp (d), TbTh (e), CtAr (f), CtTh (g) and TMD (h) in mice treated with DF ('DF'), mock miRNA ('NEG'), miR-15b, miR-365. The line in the box denotes arithmetic mean; the box denotes standard error of the mean (SEM), whiskers one standard deviation, the one-way ANOVA with Tukey's post hoc test was used, $p<0.05$ *, $p<0.01$ **

The trabecular VOI was selected beginning approximately 0.3 mm below the growth plate and extended over a 2.4 mm length, while the cortical VOI was positioned 0.6 mm above the trabecular region, continuing 0.9 mm proximally.

Dynamic Mechanical Analysis – DMA

To evaluate the macroscopic mechanical characteristics of bone samples, we employed a three-point bending protocol using the DMA 242C dynamic mechanical analyser (NETZSCH, Germany). A total of 96 femurs, distributed evenly across experimental groups (12 per group), were subjected to testing. Each thawed bone was carefully positioned within the device so that its two ends rested on supports spaced 10 mm apart while mechanical force was applied vertically at the midpoint. The test chamber temperature was programmed to increase gradually from ambient conditions to 35°C, progressing at a controlled rate of 1°C per minute.

For dynamic mechanical analysis, each specimen was exposed sequentially to six oscillation frequencies: 0.5 Hz, 1 Hz, 2 Hz, 5 Hz, 10 Hz, and 20 Hz. Each frequency was tested 16–17 times, and the average of these replicates served as a representative value for statistical processing. The full duration of a single measurement cycle was approximately 30 minutes. Consistent sample positioning was maintained throughout the experiments, and no structural failures or fractures were observed. To characterise the elastic behaviour of the examined murine femurs, we determined both the storage modulus (E′) and the loss modulus (E″). The specimens were considered to have a rectangular beam geometry, and the appropriate geometrical correction factor was applied using the formula:

$$Geometric\ factor = \frac{x^3}{4zy^3}$$

where *x* represents the span between supports, *y* the height, and *z* the width of the bone cross-section. A similar procedure was used in [16].

Cell culture, treatment and transfection

The MC3T3-E1 Subclone 4 pre-osteoblastic cell line derived from a mouse (*Mus musculus*) was obtained from ATCC (CRL-2593). Cell cultures were maintained using Minimum Essential Medium Eagle (α-MEM; Corning, Corning, NY, USA) supplemented with standard components: ascorbic acid (Avantor, Gliwice, Poland), β-glycerophosphate (Cayman Chemical, Ann Arbor, MI, USA), and antibiotics consisting of 100 U/ml penicillin, 100 µg/ml streptomycin, and 250 ng/ml amphotericin B (ABAM; Sigma, St. Louis, MO, USA). Additional reagents included fetal bovine serum (FBS; Biowest, Nuaillé, France) and trypsin/EDTA (Biowest) for cell passaging. Two types of culture media were used:

proliferation medium composed of α-MEM supplemented with 10% FBS and 1% ABAM (v/v), and differentiation medium containing α-MEM with 10% FBS, 1% ABAM (v/v), 10 mM β-glycerophosphate, and 50 μg/ml ascorbic acid. Diclofenac (DF; J62609, Alfa Aesar, Kandel, Germany), provided as diclofenac sodium salt (CAS No. 15307-79-6), was prepared as a 50 mM stock solution in sterile dimethyl sulfoxide (DMSO; DMS666, CAS No. 67-68-5; BioShop Canada Inc., Burlington, Ontario, Canada) and added to the differentiation medium at a final concentration of 50 μM.

Transfection

Lipofectamine RNAiMAX (Thermo Fisher Scientific) has been applied to transfect MC3T3-E1 cells with mmu-miR-15b-5p (Thermo Fisher Scientific, Catalog no: 4464070), mmu-miR-365-3p, (Catalog no: 4464070), negative control (mirVana™ miRNA Mimic, Negative Control no 1, 4464061, 250 nm).

Gene expression

RNA isolation and cDNA synthesis: Total RNA was isolated from cultured MC3T3-E1 cells using the TRItidy G reagent (A4051,0100; Applichem, Darmstadt, Germany) following the manufacturer's guidelines. RNA purification was subsequently performed using the High Pure Viral RNA Kit (1185882001; Roche, Mannheim, Germany). To generate cDNA, 1 μg of total RNA was reverse transcribed using the M-MLV Reverse Transcriptase Kit (5 U/μl; 28025-013, Thermo Fisher Scientific, Waltham, MA, USA). The reaction mix included RNaseOUT™ Recombinant Ribonuclease Inhibitor (10777-019, Thermo Fisher Scientific), Oligo$(dT)_{24}$ primers, 0.4 ng/μl random hexamers, 2 mM dNTPs, and 10 mM DTT. The temperature profile was as follows: 65°C for 5 minutes, rapid cooling on ice, 37°C for 50 minutes, and final inactivation at 70°C for 15 minutes. Quantitative PCR: CDNA was quantified using real-time PCR with primers specified in Table 1 of reference [18]. Amplification reactions employed the TaqMan Fast Advanced Master Mix (4444963; Thermo Fisher Scientific) and were performed on a LightCycler 96 or 480 system (Roche Diagnostics, Basel, Switzerland). Thermal cycling parameters were identical for all assays: initial incubation at 50°C for 120 seconds and 95°C for 120 seconds, followed by 45 cycles of denaturation at 95°C for 3 seconds and annealing/extension at 60°C for 30 seconds. Each reaction contained 5 μl of 2× master mix, 0.5 μl of 20× TaqMan assay, 3.5 μl of nuclease-free water, and 1 μl of cDNA. Quantification cycle (Cq) values were determined automatically using the second derivative method. Relative expression was calculated with normalisation to two reference genes, *Hprt* (hypoxanthine phosphoribosyltransferase 1) and *B2m* (β-2-microglobulin).

Statistical analysis

Statistical analyses were performed using GraphPad InStat (v7.00; GraphPad Software, San Diego, CA, USA) alongside Statistica 13.0 (TIBCO Software, Palo Alto, CA, USA). Group comparisons relied on a one-way ANOVA with Tukey's multiple-comparison post hoc test, and differences were considered significant at $p < 0.05$. Data processing also took place in Statistica for real-time PCR. First, the software automatically identified the crossing-point for each reaction via the second-derivative algorithm implemented in LightCycler 96 (v1.1.0.1320; Roche Diagnostics). Gene expression levels were then calculated against standard curves generated for each target. These values were normalised by dividing by the geometric mean of two reference genes (*Hprt* and *B2m*). Mean expression and its standard error were determined from four independent biological replicates. Control samples (no treatment, 24 h incubation) were set to a baseline value of 1. Finally, Tukey's test in Statistica 13.0 was used to confirm statistical significance. All figures and schematics were drafted in Adobe Illustrator (Adobe Inc.). The statistical approach used here is the standard methodology for studies of this kind and was previously detailed in our earlier work [18].

Results

Computer tomography

DF reduces BMD in rat tibia and femur [3]. Earlier, we published results showing that DF decreased the quality of the mouse femur, too. In our study, after four weeks of DF injection, BMD and trabecular bone volume were reduced [16]. In our current study, femurs were analysed in C57BL/6J mice injected daily with DF and once a week (four times) with miR-15b or miR-365 miRNA mimics. miRNAs were administered using an *In vivo-jetPEI* reagent because it has already been effectively applied in mice as a carrier for different siRNAs [19]. *In vivo-jetPEI* cationic polymer reagent forms nanoscale complexes with miRNAs, leading to RNA protection, cellular delivery, and intracellular release [19]. After four weeks, treated mice were terminated, and femurs were derived from soft tissues. Using the SkyScan 1172 μCT system, a microstructural analysis was performed. In Figure 1, we show results of μCT measurements of the following parameters: bone mineral density of trabecular bone (BMD), per cent bone volume (BV/TV), trabecular number (Tb.N), trabecular separation (Tb.Sp), trabecular thickness (Tb.Th), mean total cross-sectional cortical bone area (Ct.Ar), cortical cross-sectional thickness (Ct.Th) and tissue mineral density of cortical bone (TMD). We confirmed that DF decreased the BMD of the mouse femur in the trabecular bone. In our current study, NEG miRNA DF significantly decreased the BMD of trabecular bone by 30%, but BMD did not decrease in the presence of miR-15b and miR-365 (Figure 1). We

interpreted that miR-15b and miR-365 balanced the DF effect on the femur BMD. Also, we observed that the impact of miR-365 was more significant than miR-15b. Former findings indicated that miR-365 protected the osteogenesis against glucocorticoid inhibition. The protection mechanism concerns the inhibition of *Hdac4* and *Mmp-9* by miR-365 in bones [11]. These data confirm that miR-15b and miR-365 could be involved in the observed rebuilding of bone microarchitecture. In the microstructural view of the mouse femur measured by μCT, we observed a trend that miR-15b and miR-365 interplay with DF, affecting the quality of bone. These results encouraged us to investigate the biomechanical properties of bone.

DMA

We performed dynamic mechanical analysis using the DMA 242C under sinusoidal loading to evaluate the bulk mechanical behaviour of entire mouse femurs. The results—shown in Figure 2—are expressed as the bones' capacity to store energy (storage modulus, E′) and to dissipate it (loss modulus, E″), with all values reported in GPa. Throughout testing, each specimen was modelled as a simple beam and subjected to controlled oscillations while recording the force–deformation response. When diclofenac (DF) was applied alongside a non-targeting miRNA control, the bone's energy-storage capability dropped by approximately 20%. In contrast, co-treatment with either miR-15b or miR-365 completely prevented this reduction. A similar pattern emerged for viscous behaviour: DF plus control miRNA reduced the loss modulus by about 15%, but neither miR-15b nor miR-365 allowed such a decline. Thus, both miRNAs effectively neutralised diclofenac's weakening effect on bone strength. miR-15b is well established as a promoter of osteoblast maturation, and here we demonstrate its additional role in safeguarding bone mechanics against DF [8]. Likewise, miR-365—the first identified mechanically responsive miRNA involved in chondrocyte differentiation—also blocks DF-induced mechanical deterioration [20]. These findings led us to investigate whether osteoblasts themselves are the critical mediators of the protective influence exerted by miR-15b and miR-365.

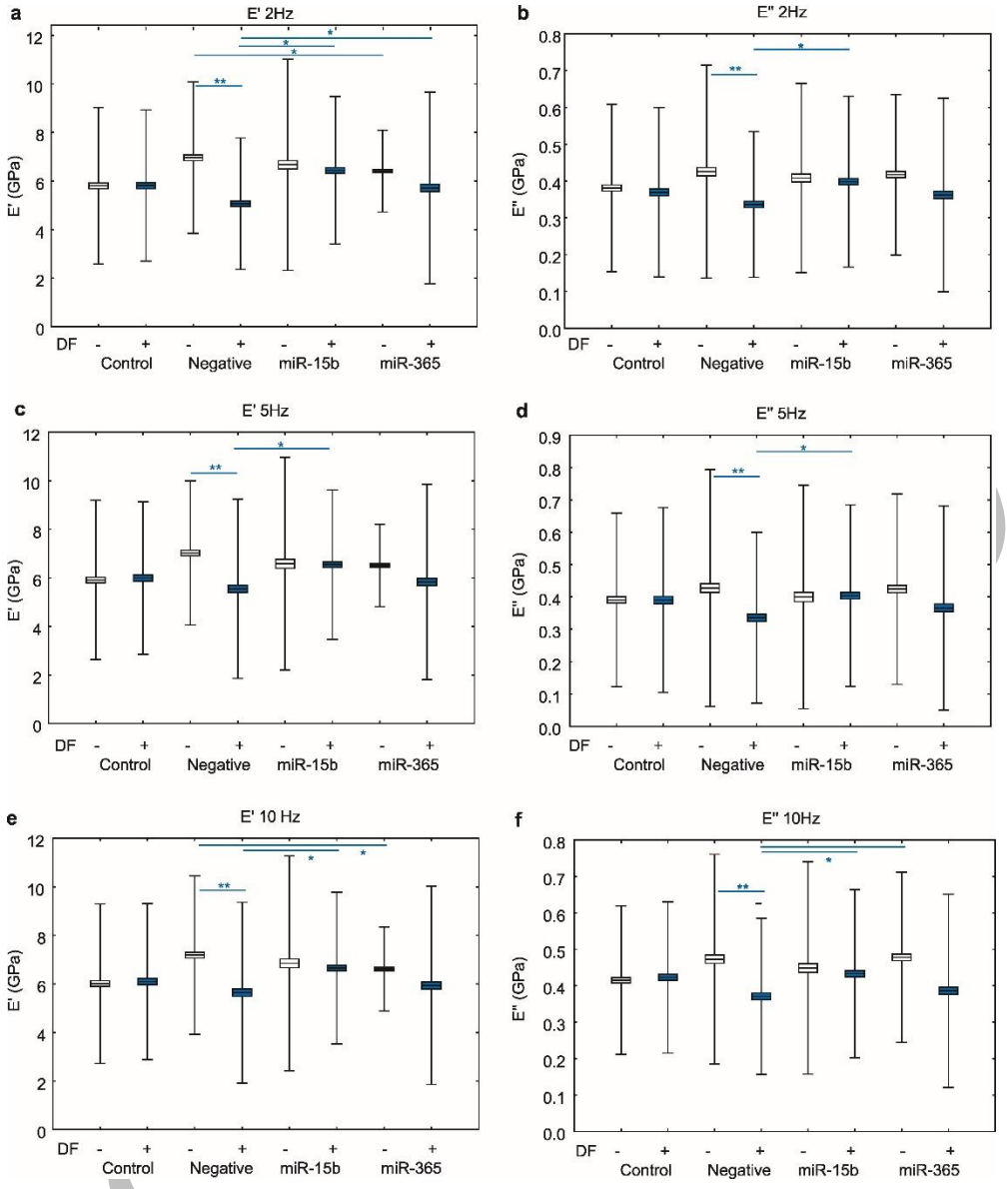

Fig.2 Mouse whole femur biomechanical assessment by dynamic mechanical analysis (DMA); E' in 2 Hz in mice treated with DF ('DF'), mock miRNA ('NEG'), miR-15b, miR-365. E'2 Hz (a), E"2 Hz (b), E'5 Hz (c), E"5 Hz (d), E'10 Hz (e), E"10 Hz (f). The line in the box denotes the arithmetic mean; the box denotes the standard error of the mean (SEM), whiskers one standard deviation, the one-way ANOVA with Tukey's post hoc test was used, $p<0.05$ *

Gene expression

Cellular sensitivity to the drug could explain changes in bone mineral density and strength during DF treatment. MC3T3-E1 cells are preosteoblast mouse calvaria cells from the C57BL/6J strain, the same model used in microstructural and DMA studies. MC3T3-E1 cells were also transfected by miR-15b and miR-365 mimics for 96 hrs. 24 hrs after transfection; we applied 50 μM DF. After RNA extraction, marker gene expression was analysed by real-

time PCR. In Figure 3, we show the results of real-time PCR for marker genes. Diagrams show relative expression to *Hprt* and *B2m*. Eight marker genes were analysed: *Osx*, *Runx2*, *Opn*, *Col1a1*, *Tgfb1*, *AlpI*, *Satb2*, and *Dlx5* in MC3T3-E1 and treated by DF. Protein products are responsible for the formation of bone structure and strength. We did not observe significant regulation of these marker genes by DF. With untreated control ('Control'), miR-15b transfection caused a decrease of *Osx*, *Runx2* and *AlpI* expression. miR-365 decreased expression *Osx*, *Runx2* and *Satb2*. DF had no impact on miR-15b and miR-365 effects.

The interaction of DF and miR-15b or miR-365 observed in mice cannot be explained by the direct interplay of DF and miRNA in preostoblasts. DF and miRNA effects should be considered on other cell types involved in bone structure and strength, like osteoclasts.

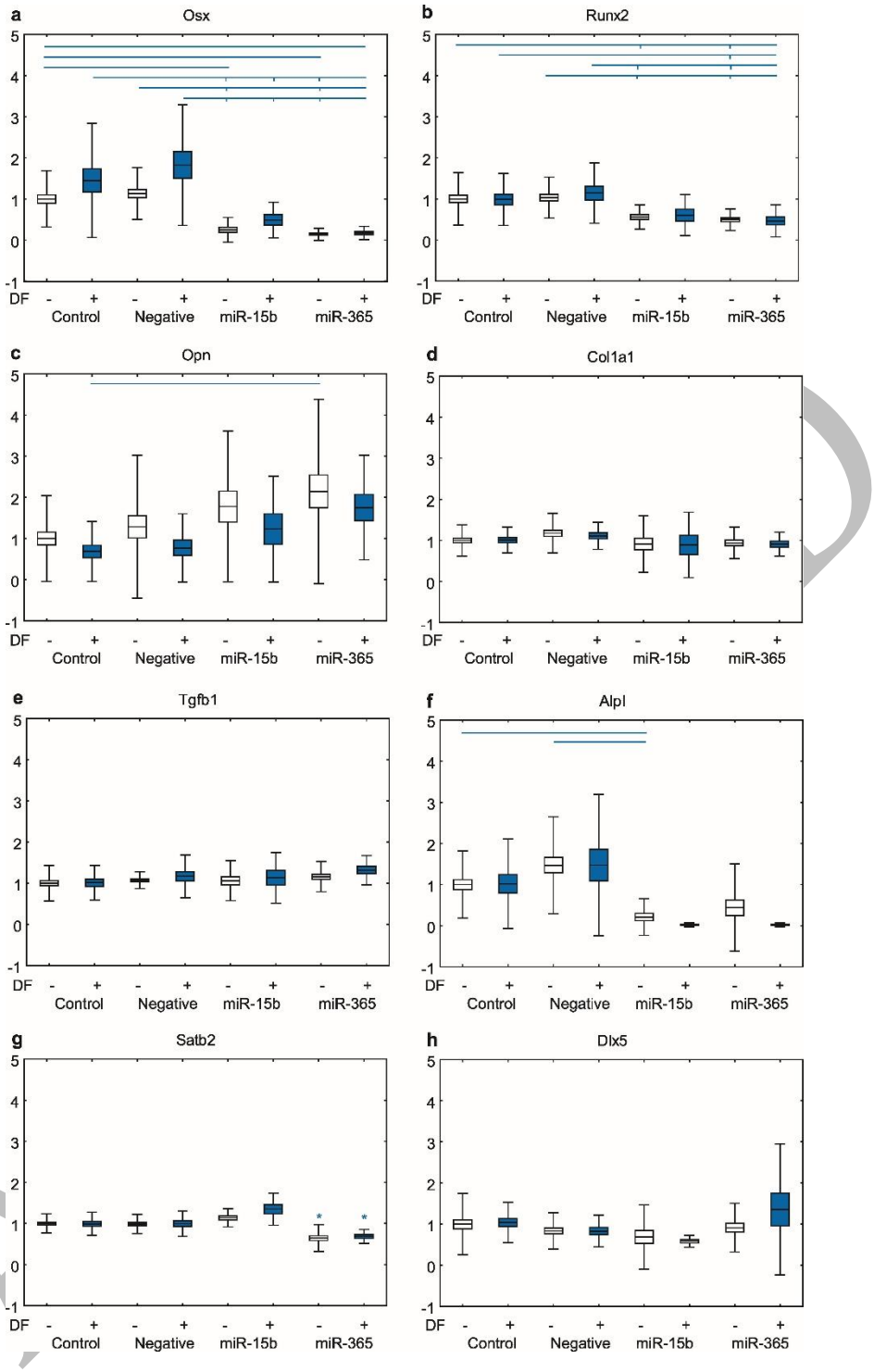

Fig.3 Gene expression analysis in MC3T3-E1 cells treated with DF, miR-15b and miR-365; Gene expression in cells treated with 50 uM DF ('DF') and transfected with mock miRNA ('NEG'), miR-15b, miR-365. *Osx* (a), *Runx2* (b), *Opn* (c), *Col1a1* (d), *Tgfb1* (e), *AlpI* (f), *Satb2* (g), and *Dlx5* (h). The line in the box denotes the arithmetic mean; the box denotes the standard error of the mean (SEM), whiskers one standard deviation, and the one-way ANOVA with Tukey's post hoc test was used.

Discussion

Numerous studies have highlighted the detrimental effects of NSAIDs on bone health in rats, mice, and humans [2]. In our previous research, we observed that DF, a specific type of NSAID, reduced mineralization in mouse femurs [16]. The current study aimed to mitigate the effects of DF by utilizing miR-15b and miR-365 mimics. While several miRNAs have been investigated as inhibitors for glucocorticoid-induced bone loss, their potential to counteract the negative effects of NSAIDs has not been explored [21, 22]. We selected miR-15b and miR-365 due to their prior examination in the context of bone physiology. Notably, miR-15b, which is transported by extracellular vesicles derived from bone marrow MSCs, promotes osteogenic differentiation [23]. We focused on miR-15b because it is abundantly expressed in differentiated osteoblasts [8]. This miRNA targets several genes, including Smurf1, Smad7, and cyclin E1, all of which play significant roles in bone cell function [7, 8, 24]. Smurf1, in particular, interacts with Runx2, a key factor in the differentiation of preosteoblasts and chondrocytes [25]. Furthermore, miR-365 has been demonstrated to reverse glucocorticoid-induced demineralization in MC3T3-E1 cells [11].

In this study, μCT analysis confirmed that DF decreases femoral mineralization in mice and increases TbSp, aligning with our previous findings [16]. DF also led to a reduction in trabecular bone thickness. Statistical analysis indicated that both miR-15b and miR-365 effectively countered the adverse effects of DF. Although DF, miR-15b, and miR-365 individually diminished bone structure, the combination of DF with either miR-15b or miR-365 mitigated these harmful effects, suggesting a reciprocal relationship between DF and these miRNAs in maintaining bone quality.

Due to the weakening of femur structure caused by DF, we assessed femoral strength using DMA. The DMA analysis corroborated the observations from μCT. DF resulted in a decrease in the bone's modulus (E'), but this effect was significantly mitigated when co-treated with miR-15b or miR-365. This indicates that DF and miRNAs may collaboratively support bone quality. Based on experiments conducted in MC3T3-E1 cells, we propose that DF does not interfere with miRNA activity at the osteoblast level, suggesting that the interaction between DF and miR-15b or miR-365 likely involves systemic mechanisms beyond osteoblasts.

In a study by Vimarlay examining human BMSC, the function of miR-15b was explored using a miR-15b inhibitor [24]. The inhibition of miR-15b in hBMSC led to a reduction in the expression of osteoblast differentiation markers such as *ALP1* and *COL1A1*, while *RUNX2* expression remained unchanged [24]. In contrast, our study found that a miR-

15b mimic decreased the expression of *Alp1*, had no effect on *Col1a1*, and reduced *Runx2* expression. This discrepancy may be attributed, in part, to differences in species and cell types utilized.

Our prior research highlighted the detrimental effects of DF on femoral bone [16], while additional studies have identified DF as an inhibitor of bone healing [3]. A potential strategy to safeguard bones from NSAID-induced damage involves the use of small RNAs. miRNA therapies have shown promise in counteracting the side effects of NSAIDs, particularly considering their role in modulating bone turnover and their correlation with bone mass abnormalities [26].

MicroRNAs (miRNAs) are emerging as promising therapeutic agents owing to their precision in synthesis and relative stability in plasma [27]. Currently, six siRNA therapeutics have received approval for clinical use, with an additional 20 under investigation [5]. Similar to glucocorticoids, valproic acid (VPA) has been shown to reduce[28] bone mineral density (BMD) [28]. However, modified extracellular vesicles (EVs) carrying miR-6359 have demonstrated the ability to protect against VPA-induced bone loss without impacting glucocorticoid-induced changes [28, 29]. While the application of miRNAs to counteract diabetic fracture (DF)-induced bone damage is a novel approach, miR-26a-5p has already been utilized in the treatment of DF-induced liver injury [30]. Numerous studies have investigated miRNA therapies aimed at alleviating the side effects of glucocorticoids on bone health. For example, miR-29a mimics have shown protective effects against glucocorticoid-induced osteoporosis [21], and miR-365 helps mitigate glucocorticoid-induced suppression of osteoblast function by downregulating *Hdac4* expression [11]. Moreover, miR-365 is also involved in regulating chondrocyte differentiation and hypertrophy [12].

This study demonstrated that miR-15b and miR-365 can protect mouse bone from damage induced by DF. Both miRNAs were found to mitigate DF-induced demineralization and loss of bone strength. Our research lays the groundwork for further investigations into miRNAs as potential protective agents against NSAID-induced bone damage. To our knowledge, this is the first study to explore miRNAs as a therapeutic approach to NSAID-induced bone toxicity. We also suggest that miR-15b and miR-365 do not directly interact with DF in osteoblast cells. The rapid advancement of miRNA-based therapies presents promising possibilities for safeguarding bones against NSAID side effects. Furthermore, miRNAs have recently been utilized in modified exosomes as carriers for targeted bone treatments [28].

It would be beneficial to confirm the *in vivo* effects of miRNAs in other bone cell types, such as osteoclasts. Future research should address the role of miRNAs in regulating systemic bone turnover, including the involvement of parathyroid hormone and other factors. Additionally, it will be vital to trace the location of miRNAs following their administration in mice and to further investigate the mechanisms by which miR-15b and miR-365 interact with DF. Developing tissue-specific delivery systems could aid in directing miRNA to osteoblasts, thereby optimizing protection against DF-induced bone damage.

Conclusions

DF decreased BMD and module E' in the mouse femur. MiR-365 alone also decreased bone module E' in mouse C57/BL femur. Moreover, miR-15b and miR-365 appeared to diminish the harmful effect of DF on bone mineral density and strength measured by the E' module. How both miRNAs interact with the DF mechanism needs to be clarified (Figure 4). Since DF did not significantly affect marker genes in MC3T3-E1 cells except *Osx/Sp7*, we concluded that DF might cause structural and biomechanical effects on bones in C57BL/6J mice based on mechanisms not involving gene expression in osteoblasts.

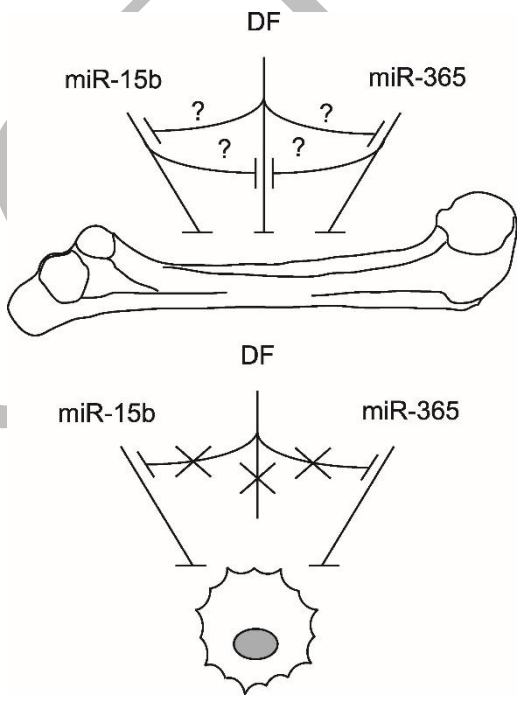

Fig.4 The schematic view of the hypothesis and results of this investigation; Using µCT, DMA and gene expression analysis methods, we tried to answer whether miR-15b and miR-365 can protect the mouse femur against the effects of diclofenac. The demineralisation of mouse femurs was protected by miR-15b and miR-365, and the mechanical properties of the bones were also improved by using miR-15b and miR-365. However, our marker gene expression measurements show that this protective effect does not occur at the level of osteoblast cells.

Acknowledgement

The Polish National Science Centre (NCN), a Polish governmental agency, funded the project under project number 2016/21/B/NZ7/02748 (OPUS 11 competition)—no commercial resources.

References:

[1] Glowacki M, Ignys-O'Byrne A, Ignys I, et al. Limb shortening in the course of solitary bone cyst treatment--a comparative study. *Skeletal Radiol* 2011; 40: 173–9.

[2] García-Martínez O, De Luna-Bertos E, Ramos-Torrecillas J, et al. Repercussions of NSAIDS drugs on bone tissue: the osteoblast. *Life Sci* 2015; 123: 72–7.

[3] Krischak GD, Augat P, Blakytny R, et al. The non-steroidal anti-inflammatory drug diclofenac reduces appearance of osteoblasts in bone defect healing in rats. *Arch Orthop Trauma Surg* 2007; 127: 453–458.

[4] Lee WY, Li N, Lin S, et al. miRNA-29b improves bone healing in mouse fracture model. *Mol Cell Endocrinol* 2016; 430: 97–107.

[5] Guo S, Zhang M, Huang Y. Three 'E' challenges for siRNA drug development. *Trends Mol Med* 2024; 30: 13–24.

[6] Bai Y, Gong X, Dong R, et al. Long non-coding RNA HCAR promotes endochondral bone repair by upregulating VEGF and MMP13 in hypertrophic chondrocyte through sponging miR-15b-5p. *Genes Dis* 2022; 9: 456–465.

[7] Fang S-H, Chen L, Chen H-H, et al. MiR-15b ameliorates SONFH by targeting Smad7 and inhibiting osteogenic differentiation of BMSCs. *Eur Rev Med Pharmacol Sci* 2019; 23: 9761–9771.

[8] Vimalraj S, Partridge NC, Selvamurugan N. A positive role of microRNA-15b on regulation of osteoblast differentiation. *J Cell Physiol* 2014; 229: 1236–44.

[9] Franceschetti T, Dole NS, Kessler CB, et al. Pathway analysis of microRNA expression profile during murine osteoclastogenesis. *PLoS One* 2014; 9: e107262.

[10] Smith SS, Kessler CB, Shenoy V, et al. IGF-I 3' untranslated region: strain-specific polymorphisms and motifs regulating IGF-I in osteoblasts. *Endocrinology* 2013; 154: 253–62.

[11] Xu D, Gao Y, Hu N, et al. miR-365 Ameliorates Dexamethasone-Induced Suppression of Osteogenesis in MC3T3-E1 Cells by Targeting HDAC4. *Int J Mol Sci*; 18. Epub ahead of print 4 May 2017. DOI: 10.3390/ijms18050977.

[12] Chen J, Wu X. Cyclic tensile strain promotes chondrogenesis of bone marrow-derived mesenchymal stem cells by increasing miR-365 expression. *Life Sci* 2019; 232: 116625.

[13] Hou C, Zhang Y, Lv Z, et al. Macrophage exosomes modified by miR-365-2-5p promoted osteoblast osteogenic differentiation by targeting OLFML1. *Regen Biomater* 2024; 11: rbae018.

[14] Murakami K, Kikugawa S, Kobayashi Y, et al. Olfactomedin-like protein OLFML1 inhibits Hippo signaling and mineralization in osteoblasts. *Biochem Biophys Res Commun* 2018; 505: 419–425.

[15] Hu N, Gao Y, Jayasuriya CT, et al. Chondrogenic induction of human osteoarthritic cartilage-derived mesenchymal stem cells activates mineralization and hypertrophic and osteogenic gene expression through a mechanomiR. *Arthritis Res Ther* 2019; 21: 167.

[16] Lehmann TP, Wojtków M, Pruszyńska-Oszmałek E, et al. Trabecular bone remodelling in the femur of C57BL/6J mice treated with diclofenac in combination with treadmill exercise. *Acta Bioeng Biomech* 2021; 23: 3–11.

[17] Leciejewska N, Pruszyńska-Oszmałek E, Mielnik K, et al. Spexin Promotes the Proliferation and Differentiation of C2C12 Cells In Vitro-The Effect of Exercise on SPX and SPX Receptor Expression in Skeletal Muscle In Vivo. *Genes (Basel)*; 13. Epub ahead of print 28 December 2021. DOI: 10.3390/genes13010081.

[18] Lehmann TP, Iwańczyk-Skalska E, Harasymczuk J, et al. Gene Expression in MC3T3-E1 Cells Treated with Diclofenac and Methylprednisolone. *Genes (Basel)*; 14. Epub ahead of print 10 January 2023. DOI: 10.3390/genes14010184.

[19] Höbel S, Aigner A. Polyethylenimines for siRNA and miRNA delivery in vivo. *Wiley Interdiscip Rev Nanomed Nanobiotechnol* 2013; 5: 484–501.

[20] Guan Y-J, Yang X, Wei L, et al. MiR-365: a mechanosensitive microRNA stimulates chondrocyte differentiation through targeting histone deacetylase 4. *FASEB J* 2011; 25: 4457–66.

[21] Ko JY, Chuang PC, Ke HJ, et al. MicroRNA-29a mitigates glucocorticoid induction of bone loss and fatty marrow by rescuing Runx2 acetylation. *Bone* 2015; 81: 80–88.

[22] Suttamanatwong S. MicroRNAs in bone development and their diagnostic and therapeutic potentials in osteoporosis. *Connect Tissue Res* 2017; 58: 90–102.

[23] Li Y, Wang J, Ma Y, et al. MicroRNA-15b shuttled by bone marrow mesenchymal stem cell-derived extracellular vesicles binds to WWP1 and promotes osteogenic differentiation. *Arthritis Res Ther* 2020; 22: 269.

[24] Vimalraj S, Selvamurugan N. Regulation of proliferation and apoptosis in human osteoblastic cells by microRNA-15b. *Int J Biol Macromol* 2015; 79: 490–7.

[25] Shen R, Chen M, Wang Y-J, et al. Smad6 interacts with Runx2 and mediates Smad ubiquitin regulatory factor 1-induced Runx2 degradation. *J Biol Chem* 2006; 281: 3569–76.

[26] Sharma AR, Lee Y-H, Lee S-S. Recent advancements of miRNAs in the treatment of bone diseases and their delivery potential. *Current research in pharmacology and drug discovery* 2023; 4: 100150.

[27] Mori MA, Ludwig RG, Garcia-Martin R, et al. Extracellular miRNAs: From Biomarkers to Mediators of Physiology and Disease. *Cell Metab* 2019; 30: 656–673.

[28] Xie X, Cheng P, Hu L, et al. Bone-targeting engineered small extracellular vesicles carrying anti-miR-6359-CGGGAGC prevent valproic acid-induced bone loss. *Signal Transduct Target Ther* 2024; 9: 24.

[29] Lehmann TP, Golik M, Olejnik J, et al. Potential applications of using tissue-specific EVs in targeted therapy and vaccinology. *Biomed Pharmacother* 2023; 166: 115308.

[30] Zhang Q, Liu Y, Yuan Y, et al. miR-26a-5p protects against drug-induced liver injury via targeting bid. *Toxicol Mech Methods* 2022; 32: 325–332.